

# Characterization of Composite Laminate Lightning Strike

## Thermal-Mechanical Coupling Damage Based on Progressive Damage

### Model

Xiao Yao<sup>1</sup>, Yin Junjie<sup>1</sup>, Li Shulin<sup>1</sup>, Yao Xueling<sup>2</sup>, Chang Fei<sup>1</sup>

<sup>1</sup>Airforce Engineering University, Xi'an, China

<sup>2</sup>Xi'an Jiao Tong University, Xi'an, China

**Keywords:** Composite laminate lightning strike coupling damage; Progressive damage model; Continuum damage mechanics (CDM); Phenomenological analysis method

**Abstract:** For the sake of characterizing composite lightning strike coupling damage, based on the method of continuum damage mechanics (CDM) and phenomenological analysis, stiffness matrix progressive damage degradation model of composite laminate structure with lightning strike ablation damage and mechanical impact damage was constructed in this paper. An effective three-dimensional finite element model (FEM) of composite laminate structure with lightning strike coupling damage has been established based on ABAQUS software, and combine UMAT subroutine, which was coded by stiffness matrix progressive damage degradation model, strength prediction and failure process analysis were accomplished under tensile load. Excellent agreement between experimental data and numerical results is observed. The results indicate that models constructed in this paper can characterize the lightning strike coupling damage well, and have the abilities to predict the residual strength and failure process of composite laminate with lightning strike coupling damage.

### Introduction

Lightning is a common natural phenomenon, an aircraft may suffer from one lightning strike between each 1000 and 10000 h of flight based on the statistics on airliner<sup>[1-2]</sup>. Recent years, composite materials are being increasingly used in the territory of aerospace due to their light weight, well mechanical properties. However, one of the main drawbacks of composites when compared with traditional metallic materials is poor electrical conductivity, about 1/1000 for aluminum alloy. So that, composite structures are easier to suffer from damage under lightning strike direct effects, and descend the strength and stiffness of composite structure.

Lightning strike damage in composite can be classified into two main categories: one is the ablation damage due to thermal decomposition of resin and sublimation of carbon fiber under the condition of extremely high temperature; another one is the mechanical impact damage due to magnetic force and acoustic pressure. Literature<sup>[3]</sup> presented the qualitative description of damage mechanism for composite subjected to lightning current. Both the ablation damage and mechanical impact damage will destroy the integrality of composite structure, and decrease its load carrying ability.

Currently, investigators had carried out some tests and simulation works with respect to composite lightning strike damage, however, most of these investigations mainly focus on lightning strike thermal ablation damage, including its form reasons, damage mode and influence factors.

Feraboli<sup>[4-5]</sup> did some test researches to investigate the damage degree and damage mode of the composite specimens with or without fastener under different peak currents by simulated lightning strike, furthermore, compared the lightning strike damage with the low velocity impact damage; Ogasawara<sup>[6]</sup> firstly presented a coupled thermal-electrical finite element analysis model based on ABAQUS thermal-electrical analysis module, to simulate lightning strike ablation damage due to resistance heating according to the transient temperature distribution in CFRP composite when exposed to simulated lightning current. Despite investigators<sup>[7-8]</sup> realized there exist lightning impact force on composite laminate panel when lightning strike occurs and also did some test to measure its magnitude, there are just a few literatures available regarding composite lightning strike mechanical impact damage. Based on ABAQUS/Explicit, author in literature<sup>[9]</sup> calculated the damage degree of carbon fiber and resin under magnetic force and acoustic pressure according to Tsai-Wu failure criteria.

According to the existing literatures, there are few researches regarding mechanical properties of composite subjected to lightning strike coupling damage. MALL S<sup>[10]</sup> test the compression strength degradation of nano-composites after lightning strike, test results just revealed the influence of ablation damage to compressive strength; Wang FS<sup>[11]</sup> calculated the tensile residual strength of composite laminate with lightning strike ablation damage through element deletion, during the simulation, author did not take the lightning strike mechanical impact damage into account.

Difficulty during researching mechanical properties of composite with lightning strike coupling damage is how to characterize the lightning strike coupling damage. At present, progressive damage analysis has become one of most popular methods to research composite impact damage and mechanical properties, which can simulate the entire material degradation process from initial failure to final destruction. Progressive damage analysis method includes fracture mechanics method<sup>[12]</sup>, continuum damage mechanics (CDM)<sup>[13]</sup> and phenomenological analysis method<sup>[14]</sup>. Take into account that lightning strike coupling damage includes ablation damage and mechanical impact damage, author presented to construct a stiffness matrix progressive damage degradation model of composite laminate structure with lightning strike coupling damage, based on continuum damage mechanics and phenomenological analysis method. An effective 3D FEM of composite laminate structure with lightning strike coupling damage has been established based on ABAQUS software, and combine UMAT subroutine, which is coded by stiffness matrix progressive damage degradation model, strength prediction and failure process analysis were accomplished under tensile load. Excellent agreement between experimental data and numerical results is observed.

## Theory

### Constitutive relationships of materials

The constitutive relationship between stress and strain for orthotropic composite materials has the form:

$$\{\sigma\} = [C]\{\varepsilon\} \quad (1)$$

Where:  $\{\sigma\} = [\sigma_1 \ \sigma_2 \ \sigma_3 \ \tau_{23} \ \tau_{12} \ \tau_{13}]^T$ ;  $\{\varepsilon\} = [\varepsilon_1 \ \varepsilon_2 \ \varepsilon_3 \ \gamma_{23} \ \gamma_{12} \ \gamma_{13}]^T$ .

$$[C] = \begin{bmatrix} C_{11} & C_{12} & C_{13} & & & \\ & C_{22} & C_{23} & & & \\ & & C_{33} & & & \\ & & & C_{44} & & \\ & sym & & & C_{55} & \\ & & & & & C_{66} \end{bmatrix} \quad (2)$$

Components in stiffness matrix  $[C]$  can be expressed by material properties as followed:

$$C_{11} = \frac{1 - \nu_{23}\nu_{32}}{E_2 E_3 \Delta}, \quad C_{12} = \frac{\nu_{21} + \nu_{31}\nu_{23}}{E_1 E_3 \Delta}, \quad C_{13} = \frac{\nu_{13} + \nu_{12}\nu_{23}}{E_1 E_2 \Delta}, \quad C_{22} = \frac{1 - \nu_{13}\nu_{31}}{E_1 E_3 \Delta}, \quad C_{23} = \frac{\nu_{23} + \nu_{21}\nu_{13}}{E_1 E_2 \Delta}, \quad C_{33} = \frac{1 - \nu_{12}\nu_{21}}{E_1 E_2 \Delta},$$

$$C_{44} = G_{23}, \quad C_{55} = G_{12}, \quad C_{66} = G_{13}, \quad \Delta = \frac{1 - \nu_{12}\nu_{21} - \nu_{23}\nu_{32} - \nu_{13}\nu_{31} - 2\nu_{21}\nu_{32}\nu_{13}}{E_1 E_2 E_3}, \quad \frac{\nu_{12}}{E_1} = \frac{\nu_{21}}{E_2}, \quad \frac{\nu_{13}}{E_1} = \frac{\nu_{31}}{E_3}, \quad \frac{\nu_{23}}{E_2} = \frac{\nu_{32}}{E_3}$$

Where  $E_i (i=1,2,3)$  is elastic modulus;  $\nu_{ij} (i=1,2,3; j=1,2,3; i \neq j)$  is Poisson's ratio;  $G_{23}, G_{31}, G_{12}$  are shear modulus.

## Composite laminate progressive damage analysis based on CDM

### Damage characterization

First of all, define the material coordinate system: 1 denotes the longitudinal direction of the fiber; 2 and 3 denote the transverse directions of the fiber. Here we adapt a second-order symmetric tensor  $D$  to define material damage, its eigenvalues  $d_i (i=1,2,3)$  represent descending degree of effective bearing area on three main directions, and also can be represented the damage variables for fiber, matrix, and delamination, respectively. The value of damage variables  $d_i$  must be in the range of 0 to 1, where  $d_i=0$  represents the perfect materials while  $d_i=1$  denotes the completely damaged materials<sup>[15]</sup>.

$$D = \begin{bmatrix} d_1 & 0 & 0 \\ 0 & d_2 & 0 \\ 0 & 0 & d_3 \end{bmatrix} \quad (3)$$

Based on CDM analysis method, once the material occur damage, the relationship between the effective stress  $[\bar{\sigma}]$  and the nominal stress  $[\sigma]$  is postulated to have the form:

$$[\bar{\sigma}] = M(D)[\sigma] \quad (4)$$

Where  $M(D)$  is the damage operator, which has the diagonal form:

$$M(D) = \text{diag} \left[ \frac{1}{k_{11}}, \frac{1}{k_{22}}, \frac{1}{k_{33}}, \frac{1}{k_{23}}, \frac{1}{k_{12}}, \frac{1}{k_{13}} \right]; \quad k_{ij} = \sqrt{(1-d_i)(1-d_j)} \quad (i, j = 1,2,3) \quad (5)$$

According to the assumption of energy equivalence:

$$W^e = \frac{1}{2} [\sigma][\varepsilon] = \frac{1}{2} [\bar{\sigma}][\bar{\varepsilon}] \quad (6)$$

Where:  $W^e$  is the elastic strain energy density;  $[\bar{\varepsilon}]$  and  $[\varepsilon]$  are the effective strain and the nominal strain, respectively.

Take Eq.(4) into Eq.(6), the elastic strain energy density can be expressed as

$$W^e = \frac{1}{2} M(D)^{-1} [\bar{\sigma}][\bar{\varepsilon}] = \frac{1}{2} [\bar{\sigma}][\bar{\varepsilon}] \quad (7)$$

According to Eq.(7), we can get the relationship between effective strain and the nominal strain:

$$[\bar{\varepsilon}] = M(D)^{-1}[\varepsilon] \quad (8)$$

Using  $[C^{d,f}]$  presents the stiffness matrix of damage material, combining Eq.(1), Eq.(7) and Eq.(8),  $[C^{d,f}]$  has the form:

$$[C^{d,f}] = M(D)^{-1}[C](M(D)^T)^{-1} \quad (9)$$

### Initial failure criteria

Hashin failure criteria<sup>[16]</sup> and Yeh delamination failure criteria<sup>[17]</sup> were selected to assess whether failure occurred at a material point. Adopting  $F_1$ ,  $F_2$  and  $F_3$  describe the initial failure criteria of fiber, resin and delamination respectively. When composite laminate has internal damage, the stresses in local damage territory distribute complexly and change violently. However, the strains' distribution changes continuous and smoothly, so, initial failure criteria based on effective strains is more suitable for describing the progressive damage evolution of composite structure. Without regard to the condition of shear nonlinearity, Hashin failure criteria and Yeh delamination failure criteria based on effective strains have the following general forms<sup>[18]</sup>:

$$F_1^2 = \begin{cases} \left(\frac{\varepsilon_{11}}{\varepsilon_1^{f,T}}\right)^2 + \left(\frac{\gamma_{12}}{\gamma_{12}^f}\right)^2 + \left(\frac{\gamma_{13}}{\gamma_{13}^f}\right)^2 \geq 1, (\varepsilon_{11} > 0) \\ \left(\frac{\varepsilon_{11}}{\varepsilon_1^{f,C}}\right)^2 \geq 1, (\varepsilon_{11} < 0) \end{cases} \quad (10)$$

$$F_2^2 = \begin{cases} \left(\frac{\varepsilon_{22} + \varepsilon_{33}}{\varepsilon_2^{f,T}}\right)^2 + \left(\frac{1}{(\gamma_{23}^f)^2}\right)(\gamma_{23}^2 - \frac{E_2 E_3}{G_{23}} \varepsilon_{22} \varepsilon_{33}) + \left(\frac{\gamma_{12}}{\gamma_{12}^f}\right)^2 + \left(\frac{\gamma_{13}}{\gamma_{13}^f}\right)^2 \geq 1, (\varepsilon_{22} + \varepsilon_{33} > 0) \\ \left(\frac{E_2 \varepsilon_{22} + E_3 \varepsilon_{33}}{2G_{12} \gamma_{12}^f}\right)^2 + (\varepsilon_{22} + \varepsilon_{33}) \left[ \frac{E_2 \varepsilon_2^{f,C}}{2G_{12} \gamma_{12}^f} - 1 \right] + \frac{1}{(\gamma_{23}^f)^2} (\gamma_{23}^2 - \frac{E_2 E_3}{G_{23}} \varepsilon_{22} \varepsilon_{33}) \\ + \left(\frac{\gamma_{12}}{\gamma_{12}^f}\right)^2 + \left(\frac{\gamma_{13}}{\gamma_{13}^f}\right)^2 \geq 1, (\varepsilon_{22} + \varepsilon_{33} < 0) \end{cases} \quad (11)$$

$$F_3^2 = \begin{cases} \left(\frac{\varepsilon_{33}}{\varepsilon_3^{f,T}}\right)^2 + \left(\frac{\gamma_{13}}{\gamma_{13}^f}\right)^2 + \left(\frac{\gamma_{23}}{\gamma_{23}^f}\right)^2 \geq 1, (\varepsilon_{33} > 0) \\ \left(\frac{\gamma_{13}}{\gamma_{13}^f}\right)^2 + \left(\frac{\gamma_{23}}{\gamma_{23}^f}\right)^2 \geq 1, (\varepsilon_{33} < 0) \end{cases} \quad (12)$$

In the above equations,  $\varepsilon_{ii} (i=1,2,3)$  is the normal strain in  $i$  direction;  $\gamma_{12}$ ,  $\gamma_{13}$  and  $\gamma_{23}$  are the shear strains in 1-2, 1-3, and 2-3 planes, respectively.  $\varepsilon_i^{f,T}$  or  $\varepsilon_i^{f,C}$  ( $i=1,2,3$ ) represents tensile and compressive normal strain strength in  $i$  direction,  $\gamma_{12}^f$ ,  $\gamma_{13}^f$  and  $\gamma_{23}^f$  denote shear strain strength in 1-2, 1-3, and 2-3 planes:

$$\varepsilon_1^{f,T} = \frac{X_T}{C_{11}}, \varepsilon_1^{f,C} = \frac{X_C}{C_{11}}, \varepsilon_2^{f,T} = \frac{Y_T}{C_{22}}, \varepsilon_2^{f,C} = \frac{Y_C}{C_{22}}, \varepsilon_3^{f,T} = \frac{Z_T}{C_{33}}, \varepsilon_3^{f,C} = \frac{Z_C}{C_{33}}, \gamma_{12}^f = \frac{S_{12}}{C_{44}}, \gamma_{13}^f = \frac{S_{13}}{C_{55}}, \gamma_{23}^f = \frac{S_{23}}{C_{66}}$$

### Damage evolution

In the initial failure criteria, when  $F_i$  is less than one, the material is undamaged. When  $F_i$  equal one, the material is damaged, and further loading will cause degradation of material stiffness coefficients, at this time, adopting the degradation model of material properties based on exponential material damage evolution law, calculation formula for damage state variables can be described as<sup>[19]</sup>:

$$d_i = 1 - \frac{\exp(C_{ii}(\varepsilon_i^f)^2 L^c (1 - F_i) / G_i^C)}{F_i} \quad i = 1, 2, 3 \quad (13)$$

Where  $L^c$  is the characteristic length of the finite element, which can reduce the mesh sensitivity during the stage of damage evolution;  $G_i^C$  denote the critical fracture dissipation energies in three main material directions, respectively.

**Characterization of composite laminate lightning strike coupling damage  
Material properties degradation model due to lightning strike ablation damage**

The internal resin decomposed gases will expand rapidly, under the act of which the bareness carbon fiber will be fractured, sketch map is shown in Fig.1. Based on the above perspective, author puts forward material properties degradation model due to lightning strike ablation damage as followed: when the temperature lower than thermal decomposition initial temperature, composite material properties remain the same to origin; when the temperature locate in the range of thermal decomposition temperature, composite material properties change linearly with the degree of decomposition; when the temperature higher than the thermal decomposition termination temperature, composite material properties is zero, but for the sake of improving the convergence of simulation, we assume the composite material properties is 0.001times as much as initial material properties.

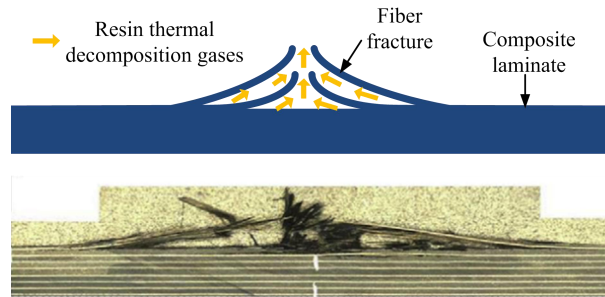


Fig. 1. Fractured carbon fiber under the act of resin thermal decomposition gases

Set parameter  $K$  as the composite initial material property (just take elastic modulus and shear modulus change with degree of decomposition into account),  $t_0$  is the thermal decomposition initial temperature;  $t_1$  is the thermal decomposition termination temperature. During the whole temperature rising process, composite material properties can be expressed as:

$$K = \begin{cases} K & (t \leq t_0) \\ (1 - \alpha(T))K & (t_0 < t \leq t_1) \\ 0.001K & (t > t_1) \end{cases} \quad (14)$$

Where  $\alpha(T)$  denotes resin decomposition degree, the rate of decomposition is determined by the temperature,  $T$ . The following empirical equation is often applied for estimating the decomposition kinetics for a thermosetting resin<sup>[20]</sup>.

$$\frac{d\alpha}{dT} = \frac{A}{\beta} \exp\left(-\frac{E_a}{RT}\right) (1 - \alpha)^n \quad (15)$$

Where  $A$  is the pre-exponential factor,  $E_a$  is the activation energy,  $R$  is the universal gas constant ( $R=8.314 \text{ J/mol/K}$ ),  $\beta$  is a constant heating rate,  $n$  is the reaction order.

Eq.(15) can be integrated by the separation of variables method such that<sup>[21]</sup>:

$$g(\alpha) = \int_0^\alpha \frac{d\alpha}{(1 - \alpha)^n} = \frac{A}{\beta} \int_{t_0}^{t_1} \exp\left(-\frac{E_a}{RT}\right) dT \quad (16)$$

Solve Eq.(16) to get the expression of  $\alpha$ .

$$\alpha = 1 - \exp\left[ \frac{1}{1 - n} \ln\left\{ 1 - (1 - n) \int_{t_0}^t \frac{A}{\beta} \exp\left(-\frac{E_a}{RT}\right) dT \right\} \right] \quad (17)$$

Now, the degree of decomposition is expressed as a function of temperature.

**Characterization of lightning strike ablation damage**

The existence of ablation damage will induce degradation of material properties, and chapter

gives the material properties degradation model due to ablation damage. So, according to phenomenological analysis method, we can characterize the lightning strike ablation damage base on constructing the stiffness matrix progressive damage degradation model of composite laminate structure with ablation damage. Set matrix  $[C^{d,s}]$  as the stiffness matrix of composite laminate with ablation damage, combing Eq.(2) and Eq.(14), it can be expressed as:

$$[C^{d,s}] = \begin{cases} [C] & (t \leq t_0) \\ (1 - \alpha(T))[C] & (t_0 < t \leq t_1) \\ 0.001[C] & (t > t_1) \end{cases} \quad (18)$$

In order to keep material properties at temperature  $t_1$  consist with material properties when temperature higher than  $t_1$ , maximum value of  $\alpha(T)$  is 0.999.

### **Characterization of lightning strike coupling damage**

According to the previous analysis, under the act of lightning strike, composite structure has ablation damage and mechanical impact damage at the same time. Chapter 2.2.1 and chapter 2.3.1 have given the expressions to characterize the lightning strike mechanical impact damage and ablation damage respectively. Set matrix  $[C^d]$  as the stiffness matrix of composite laminate with lightning strike coupling damage, combing Eq.(9) and Eq.(18), it can be expressed as:

$$[C^d] = \begin{cases} M(D)^{-1}[C](M(D)^T)^{-1} & (t \leq t_0) \\ (1 - \alpha(T))M(D)^{-1}[C](M(D)^T)^{-1} & (t_0 < t \leq t_1) \\ 0.001M(D)^{-1}[C](M(D)^T)^{-1} & (t > t_1) \end{cases} \quad (19)$$

So ,constitutive equation of composite structure with lightning strike coupling damage has the form:

$$\{\sigma\} = [C^d] \{\varepsilon\} \quad (20)$$

### **Finite element analysis**

Finite element analysis process can be divided into three steps: first, based on ABAQUS thermal-electrical analysis module, calculating the transient temperature field during lightning strike and combining the thermal decomposition behavior of resin, to simulate the CFRP composite lightning strike ablation damage due to resistance heating; second, based on ABAQUS/Explicit and combining VUMAT user subroutine, to simulate the composite lightning strike mechanical impact damage; third, based on ABAQUS/Standard and combining UMAT user subroutine, to predict residual strength and analyze failure process under tensile load for composite laminate with lightning strike coupling damage, during this step, regard the transient temperature field result in first step as the predefined temperature field, at the same time, regard the mechanical impact damage state variables result in second step as the initial state.

#### **Analytical model**

Construct simulation model based on the test in literature<sup>[5]</sup>, including material, specimen size, boundary conditions and current load, for the sake of confirming the accuracy of the model. Carbon fiber/epoxy composite is HTA/7714A, with a 16-ply quasi-isotropic layup  $[(45/0_2/-45/0_3/90)_S]$ , specimen size is  $304.8\text{mm} \times 38.1\text{mm} \times 2.88\text{mm}$ , the thickness of each ply is 0.18mm. Take the coupled thermal-electrical analysis into account, during constructing the FE model, refine the mesh at the center of the composite laminate. Total number of simulation elements is 43200. Material properties, such as thermal conductivity, electrical conductivity, specific heat and density are given in Table 1, which are dependent on the temperature. Composite engineering material parameters, such as modulus, Poisson's ratios, strength and critical fracture dissipation energies are given in Table 2.

**Table 1** Composite thermal and electrical material properties vs. temperature[8]

| Temperature (°C) | Density (kg/mm <sup>3</sup> ) | Specific heat (J/kg°C) | Longitudinal thermal conductivity (W/mm°C) | Transverse thermal conductivity (W/mm°C) | Longitudinal electrical conductivity (1/Ωmm) | Transverse electrical conductivity (1/Ωmm) | In depth electrical conductivity (1/Ωmm) |
|------------------|-------------------------------|------------------------|--|--|--|--|--|
| 25               | 1.52e-6                       | 1065                   | 0.008                                      | 0.00067                                  | 35.97  | 0.001145                                   | 3.876e-6                                 |
| 343              | 1.52e-6                       | 2100                   | 0.02608                                    | 0.00018                                  | 35.97  | 0.001145                                   | 3.876e-6                                 |
| 500              | 1.1e-6                        | 2100                   | 0.001736                                   | 0.0001                                   | 35.97  | 2  | 2  |
| 510              | 1.1e-6                        | 1700                   | 0.001736                                   | 0.0001                                   | 35.97  | 2  | 2  |
| 1000             | 1.1e-6                        | 1900                   | 0.001736                                   | 0.0001                                   | 35.97  | 2  | 2  |
| 3316             | 1.1e-6                        | 2509                   | 0.001736                                   | 0.0001                                   | 35.97  | 2  | 2  |
| >3316            | 1.1e-6                        | 5875                   | 0.00105                                    | 0.001015                                 | 0.2  | 0.2  | 1e6                                      |

**Table 2** Composite engineering material parameters[23]

| $E_1$ | $E_2$ | $E_3$ | $\nu_{12}$ | $\nu_{13}$ | $\nu_{23}$ | $G_{12}$ | $G_{13}$ | $G_{23}$ | $X_T$   | $X_C$ |
|-------|-------|-------|------------|------------|------------|----------|----------|----------|---------|-------|
| /GPa  | /GPa  | /GPa  |            |            |            | /GPa     | /GPa     | /GPa     | /MPa    | /MPa  |
| 137   | 8.2   | 8.2   | 0.3        | 0.3        | 0.45       | 4.36     | 4.36     | 3        | 1708    | 1251  |
| $Y_T$ | $Y_C$ | $Z_T$ | $Z_C$      | $S_{12}$   | $S_{13}$   | $S_{23}$ | $G_1^C$  | $G_2^C$  | $G_3^C$ |       |
| /MPa  | /MPa  | /MPa  | /MPa       | /MPa       | /MPa       | /MPa     | N/mm     | N/mm     | N/mm    |       |
| 34    | 192   | 34    | 192        | 128        | 128        | 96       | 20       | 1        | 1       |       |

**Lightning strike ablation damage analysis**

Simulating the lightning strike ablation damage of composite through coupled thermal-electrical analysis based on ABAQUS thermal-electrical analysis module, element type is DC3D8E. In order to simulate the true test environment, boundary conditions of the simulation model are as follow: electrical potential of the both ends surfaces are assumed to be zero due to electrically grounded; thermal radiation will occur because of transient heat transmit of the specimen, assuming the upper and side surfaces radiate heat and the bottom surface is adiabatic, the emissivity is 0.9 and the environment temperature is 25°C.

In order to compare the simulation results with test results in literature[5], the current intensity vs. time waveforms for all three strike levels are shown in Fig.2

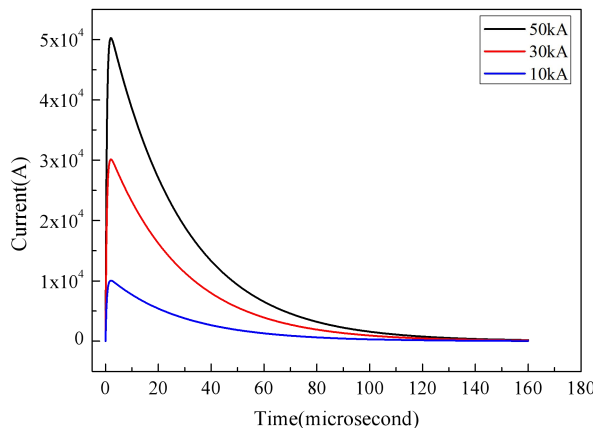


**Fig. 2.** Lightning current waveforms

**Lightning strike mechanical impact damage analysis**

The magnitude of the magnetic force comes from the direct application of the Maxwell equations to a current of intensity  $I(t)$  with a column radius  $R_c$  injected in an infinite flat panel. The

magnetic force field  $p(r, t)$  that acts on the panel can be computed as [3][9]:

$$p(r, t) = \begin{cases} \frac{\mu_0 I^2(t)}{4\pi^2 R_c^2} & r < R_c \\ \frac{\mu_0 I^2(t)}{4\pi^2 r^2} & r > R_c \end{cases} \quad (21)$$

Where  $r$  is the radial distance to the lightning attachment point,  $\mu_0 = 4\pi \times 10^{-7}$  N/A is the magnetic permeability and  $t$  is the time. Arc radius of  $R_c = 5$  mm.

Simulating the lightning strike mechanical impact damage of composite based on ABAQUS/Explicit, element type is C3D8R. Both ends of the laminate were fixed as the displacement boundary conditions, and then apply magnetic force and acoustic pressure based on Eq.(21) and Fig.3 at the lightning strike attachment point and nearby region, combing VUMAT user subroutine, calculating the damage degree of fiber, resin and delamination under the act of lightning strike mechanical impact.

### Strength prediction and failure process analysis

Assessment the residual strength and failure process of composite laminate with lightning strike coupling damage based on ABAQUS/Standard, element type is C3D8R. One side of the laminate is fixed and another one applies a displacement load as the boundary conditions. Regard the transient temperature field result in chapter 3.2 as predefined temperature field. At the same time, regard the mechanical impact damage state variables result in chapter 3.3 as the initial state. Combing UMAT user subroutine, calculate the tensile residual strength and analyze the failure process.

## Results and discussion

### Lightning strike coupling damage analysis results

#### Ablation damage analysis results

Value of composite resin decomposition kinetic parameter in Eq.(17) presented as followed:  $n=3.5$ ,  $A=5.0 \times 10^{13}$  (1/min),  $E_a=180$ (kJ/mol/K)[6]. Based on Eq.(17), we can get the decomposition degree curves of resin under different temperature rising rate (5°C/min., 10°C/min., 20°C/min., 50°C/min. and 100°C/min), which is shown in Fig.3. From Fig.3, it can be seen that temperature range of resin thermal decomposition is about 250°C ~700°C. Resin initial decomposition behavior can be regarded as damage criteria, that is to say, temperature profile greater than 250°C of simulation result can represent ablation damage.

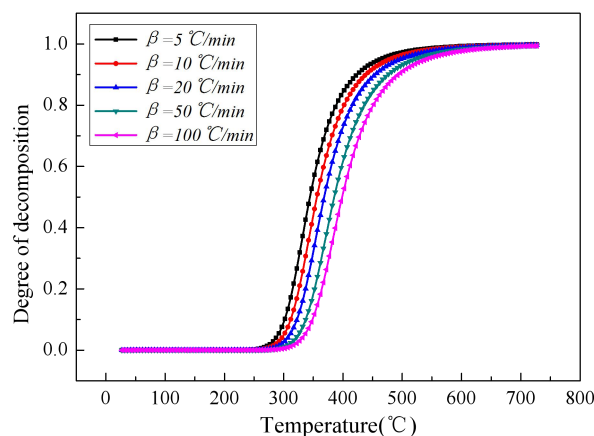


Fig. 3. Degree of decomposition curves of resin under different temperature rising rate

Fig.4 shows damage distribution image of test specimen, Ultrasonic C-scan nondestructive examination and simulation under the peak current of 30kA. Compared Fig.4 (a) with Fig.4 (c), damage in the outermost layer propagate along the fiber direction (45°) both the test result and

simulation result; Compared Fig.4 (b) with Fig.4 (c), the damage image of ultrasonic C-scan and simulation can be well matched. (Notice that: Fiber direction of first layer in simulation model is  $45^\circ$  , but that of test specimen is  $-45^\circ$  ). Table 3 shows the damage area compared between test results and simulation results under different peak current. From the compared results in Table 3, ablation damage area of the simulation results agree with that of test results well, all of the errors are less than 10%.

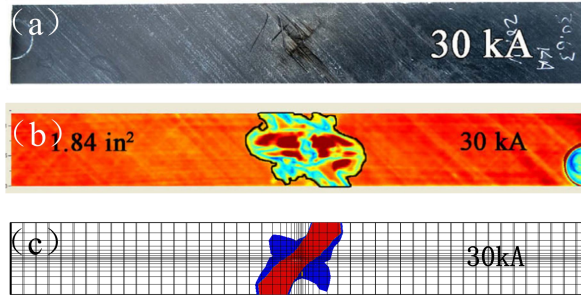


Fig. 4. Damage appearance image compared between test and simulation from overhead view

Table 3 Damage area compared between test results and simulation results under different peak current

| Peak current<br>/kA | Test results<br>/mm <sup>2</sup> | Simulation results<br>/mm <sup>2</sup> | $E_{\text{error}}/\%$ |
|---------------------|----------------------------------|--|-----------------------|
| 10                  | 658                              | 618                                    | 6.08                  |
| 30                  | 1187                             | 1102                                   | 7.16                  |
| 50                  | 1567                             | 1505                                   | 3.96                  |

### Mechanical impact damage analysis results

In this section, lightning strike mechanical impact damage under different peak current has been analyzed. According to Table 4, we can see that, under the test given support conditions, accompany with the increasing of peak current, mechanical impact damage degree will be increased gradually. When the peak current less than 50kA, under the act of mechanical impact, values of damage variables are zero. When the peak current higher than 50kA, resin appeared damage firstly, accompany with the increasing of peak current, fiber damage and delamination damage appeared gradually.

Table 4 Mechanics damage degree under different peak current

| Peak current<br>/kA | $d_1$ | $d_2$ | $d_3$ |
|---------------------|-------|-------|-------|
| 10                  | 0     | 0     | 0     |
| 30                  | 0     | 0     | 0     |
| 50                  | 0     | 0     | 0     |
| 75                  | 0     | 0.41  | 0     |
| 100                 | 0     | 0.60  | 0     |
| 150                 | 0.1   | 0.79  | 0.05  |
| 200                 | 0.67  | 0.87  | 0.28  |

The distribution of lightning strike mechanical impact damage in section A-A of the laminate under the peak current of 200kA is presented in Fig.5. It can be seen that, fiber damage and resin damage mainly distribute in the bottom several layers, delamination damage distribute in the upper several layers, and its damage territory is smallest.

Combing Table 4 and Fig.5, we can see that, under the act of lightning strike mechanical impact, although there is no visible damage, stiffness matrix already degrade due to the existence of damage

variables, it will affect the composite loading carrying capacity to some extent, so, just take ablation damage into account when evaluate the residual strength and analyze failure process is not enough, must take the mechanical impact damage into account as well.

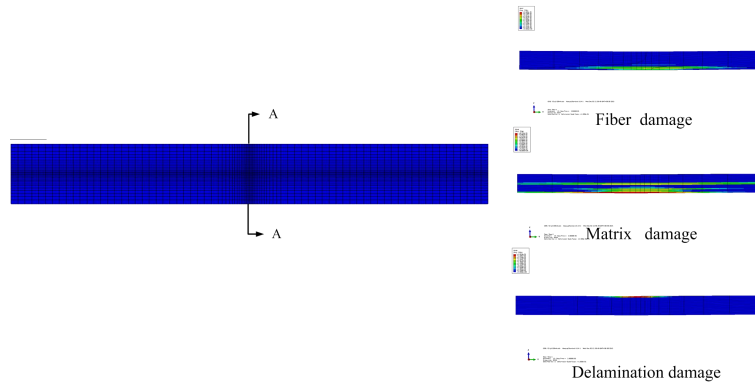


Fig. 5. Damage distribution in section A-A

### Tensile strength prediction results

In this part, tensile residual strength of composite with lightning strike coupling damage is calculated. Fig. 6 shows the simulation tensile load-displacement curves of composite which have been subjected to different peak current, include 0kA, 10kA, 30kA and 50kA, 0kA represent undamaged specimen. Damage load and damage displacement under different peak current are shown in Table 5. According to Fig.6 and Table 5, we can see that accompany with increasing of peak current, both the simulation results of damage load and damage displacement are descend linearly. Simulation results in chapter 4.1.1 show that, lightning strike damage area increase with the increasing of peak current, so, degree of stiffness matrix degradation is more serious and lead to the decline of residual strength. Table 4 presented that, there is no lightning strike mechanical impact damage exist in composite laminate when the peak current less than 50kA, so, the decline of residual strength in Table 5 is caused by ablation damage.

Table 5 Simulation result of damage loading and displacement under different peak current

| Peak current /kA | Damage load /kN | Damage displacement /mm | Descend percentage of load carrying capacity |
|------------------|-----------------|-------------------------|--|
| 0                | 123             | 3.76                    | /  |
| 10               | 117             | 3.61                    | 4.87   |
| 30               | 100             | 3.10                    | 18.70  |
| 50               | 93.4            | 2.98                    | 24.06  |

In order to confirm the accuracy of the simulation results, Table 6 shows the damage load compared between test results<sup>[5]</sup> and simulation results under different peak current.

Table 6 Damage load compared between test results and simulation results under different peak current

| Peak current /kA | Test results /kN | Simulation results /kN | $E_{error}/\%$ |
|------------------|------------------|------------------------|----------------|
| 0                | 126              | 123.2                  | 2.38           |
| 10               | 127              | 117                    | 7.87           |
| 30               | 104              | 100                    | 3.84           |
| 50               | 98               | 93.4                   | 4.69           |

According to Table 6, we can see that errors of damage load compared between test results and

simulation results under different peak current except for 10kA are all less than 5%. During the test<sup>[5]</sup>, the dispersion of test result under the act of 10kA is larger than others, average results of damage load is even higher than undamaged specimen. So, compared results indicate that models constructed in this paper can characterize the lightning strike coupling damage well, and have the ability to predict the residual strength of composite laminate with lightning strike coupling damage.

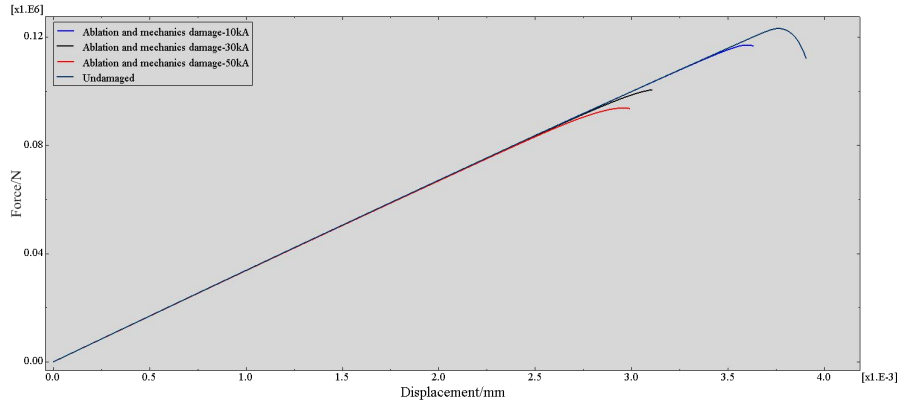


Fig. 6. Load–displacement curves under different peak current

As previous analysis mentioned, there is no lightning strike mechanical impact damage exist in composite laminate when the peak current less than 50kA. In order to investigate influence of mechanical impact damage to composite residual strength, in this section, calculate the composite tensile residual strength under the act of ablation damage and coupling damage respectively, and peak current is 100kA. Fig. 8 shows the simulation tensile load- displacement curves.

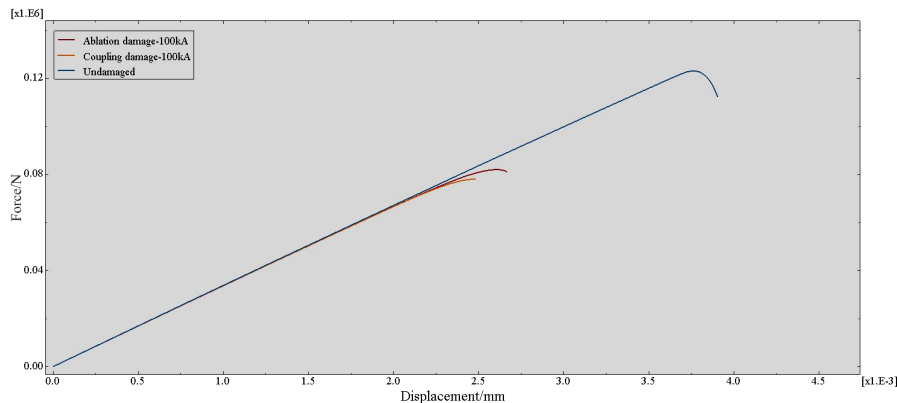


Fig. 7. Load–displacement curves under ablation damage and coupling damage

Table 7 Simulation result of damage load and displacement under ablation damage and coupling damage

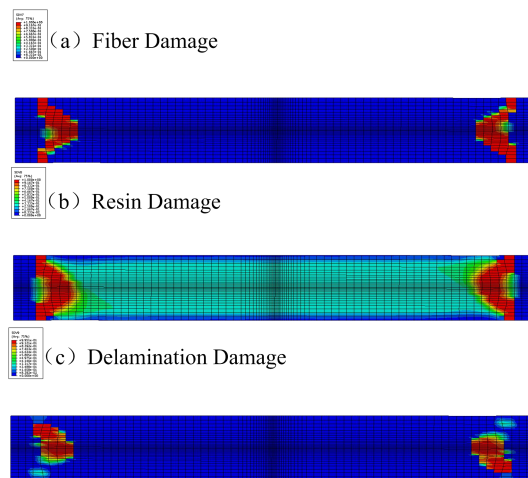
| Damage model    | Damage load /kN | Damage displacement /mm | Descend percentage of load carrying capacity |
|-----------------|-----------------|-------------------------|--|
| Undamaged       | 123.2           | 3.76                    | /  |
| Ablation damage | 82.1            | 2.60                    | 33.3   |
| Coupling damage | 78.1            | 2.48                    | 36.6   |

Table 7 shows the simulation result of damage load and displacement under ablation damage and coupling damage. Compared the damage load between ablation damage and coupling damage, we can see that, damage load under the act of ablation damage is higher than that of coupling damage about 4.87%, and total descend percentage of load carrying capacity is greater than 30%. So,

simulation results indicate that, both ablation damage and mechanical impact damage will reduce the composite tensile residual strength, and the ablation damage plays a leading role.

**Failure process analysis results**

Lightning strike coupling damage not only affects composite tensile residual strength, but also changes the failure process of composite laminate. It can be seen from Fig.8 that undamaged specimen under tensile load, its failure location locates at both ends of the laminate. Because of fiber plays a leading role when laminate subjected to tensile load, fiber damage evolution process under tensile load is depicted in Fig.9. At the same time, Fig.10 shows the sketch map of fiber damage propagation. Combing Fig.9 and Fig.10, we can see that, initial fiber damage start at location A1 and A2 in Fig.10, and then propagated along the  $-45^\circ$  and  $+45^\circ$  directions respectively accompany with the increasing tensile load, at last, fiber damages intersect at location B in Fig.10, and rising continuous last to structure failure completely.



**Fig. 8.** Damage distribution of specimen without lightning strike coupling damage

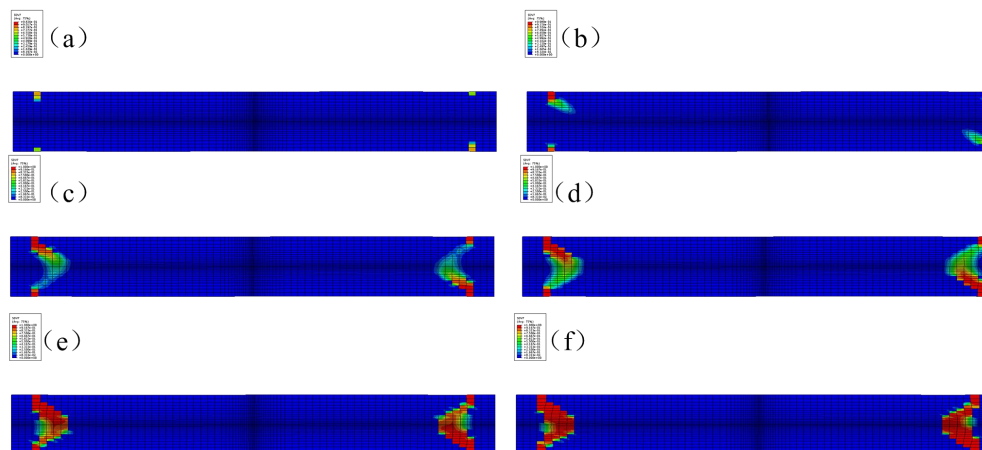


**Fig. 9.** Fiber damage evolution process of specimen without lightning strike coupling damage

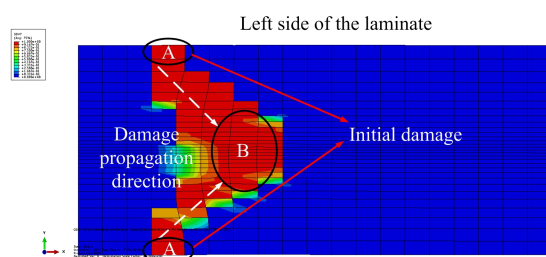


**Fig. 10.** Sketch map of undamaged specimen fiber damage propagation

Due to the existence of the lightning strike coupling damage, stress distribution in the laminate was changed compared with perfect specimen. In the ablation damage territory and mechanical impact damage territory, composite stiffness was declined, and can not bear enough load, so, stress concentration exist around the boundaries of damage territory, which is shown in Fig.11, under the act of stress concentration, fiber around the boundaries of damage territory appear damage firstly, and then propagated continuously

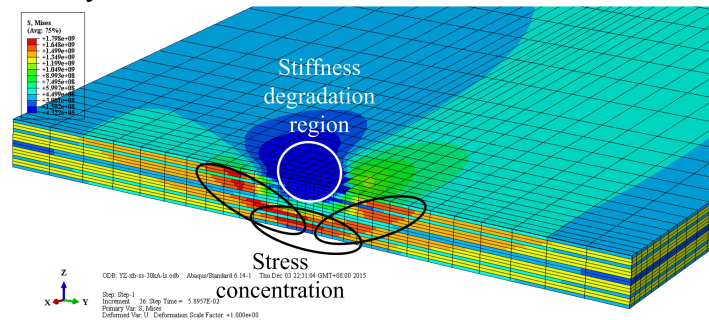


Fig. 11 Sketch map of stress concentration

## Conclusions

Based on the method of continuum damage mechanics and phenomenological analysis, author constructs stiffness matrix progressive damage degradation model of composite laminate structure with lightning strike coupling damage, to characterize lightning strike coupling damage. An effective 3D FEM of composite laminate structure with lightning strike coupling damage has been established based on ABAQUS software, and combine UMAT subroutine, strength prediction and failure process analysis were accomplished under tensile load, the numerical results correlate well with the test results of Feraboli P<sup>[5]</sup>, errors of tensile residual strength between test and simulation are less than 5%. Compared between ablation damage and mechanical impact damage, the former has larger influence on composite tensile load carrying capability. Due to the existence of lightning strike coupling damage, stress distribution in laminate was changed compared with perfect specimen, and then, failure process of composite laminate was also changed. Under the act of tensile load, failure locations of composite laminate without lightning strike coupling damage locate at both ends of the laminate, but for composite laminate with lightning strike coupling damage, its failure locations locate at the ablation damage territory of the laminate.

## Acknowledgement

This study is supported by the National Natural Science Foundation (No: 51477132).

## Reference

- [1]. Uman MA , Rakov VA. The interaction of lightning with airborne vehicles. *Prog Aerosp Sci* 2003; 39: 61–81.
- [2]. Gagne M, Therriault D. Lighting strike protection of composites. *Prog Aerosp Sci* 2014; 64: 1–16.
- [3]. Chemartin L, Lalande P, Peyrou B. Direct effects of lightning on aircraft structure: analysis of the thermal, electrical and mechanical constraints. *J Aerospace Lab* 2012 (5).
- [4]. Feraboli P, Kawakami H. Damage of carbon/epoxy composite plates subjected to mechanical

- impact and simulated lightning. *J Aircr* 2010; 47: 999–1012.
- [5]. Feraboli P, Miller M. Damage resistance and tolerance of carbon/epoxy composite coupons subjected to simulated lightning strike. *Compos: Part A* 2009; 40: 954–967.
- [6]. Ogasawara T, Hirano Y, Yoshimura A. Coupled thermal–electrical analysis for carbon fiber/epoxy composites exposed to simulated lightning current. *Compos: Part A* 2010;41: 973–983.
- [7]. Haigh Taylor SJ. Impulse effects during simulated lightning attachments to lightweight composite panels. Int Aerospace Ground Conf Lightning Static Electricity. Paris; 2007.
- [8]. Lepetit B, Escure C, Guinard S, Revel I, Peres G. Thermo-mechanical effects induced by lightning on carbon fibre composite materials. Int Aerospace Ground Conf Lightning Static Electricity. Pars; 2011.
- [9]. Munoz R, Delgado S, Gonzalez C, et al. Modeling Lightning Impact Thermo-Mechanical Damage on Composite Materials. *Appl Compos Mater* 2014;21: 149–164.
- [10]. MALL S, OUPER B L. Compression Strength Degradation of Nanocomposites after Lightning Strike. *J Compos Mater* 2009; 0: 1–15.
- [11]. Wang FS, Ding N, Liu ZQ, et al. Ablation damage characteristic and residual strength prediction of carbon fiber/epoxy composite suffered from lightning strike. *Compos struct* 2014;117: 222–233.
- [12]. Costa J, Turon A, Trias D, et al. A progressive damage model for unidirectional fibre-reinforced composites based on fiber fragmentation. Part II: Stiffness reduction in environment sensitive fibers under fatigue. *Compos Sci Technol* 2005;65: 2269–2275.
- [13]. Liu PF, Zheng JY. Progressive failure analysis of carbon fiber/epoxy composite laminates using continuum damage mechanics. *Mat Sci Eng A-Struct* 2008; 485: 711–717.
- [14]. Tserpes KI, Labeas G, Papanikos P, et al. Strength prediction of bolted joints in graphite/epoxy composite laminates. *Compos Part B* 2002; 33: 521-529 .
- [15]. Wang Y, Tong M, Zhu S. Three dimensional continuum damage mechanics model of progressive failure analysis in fiber-reinforced composite laminates[C]//50th AIAA/ASME/ASCE/AHS Structures, Structure Dynamics, and Materials Conference. California: Palm Springs, 2009.
- [16]. Hashin Z. Failure criteria for unidirectional fiber composites. *J Appl Mech* 1980; 47: 329–334.
- [17]. Yeh HY, Kim CH. The Yeh–Stratton criterion for composite materials. *J Compos Mater* 1994; 28: 926–39.
- [18]. Chien-Hua Huang, Ya-Jung Lee. Experiments and simulation of the static contact crush of composite laminated plates. *Compos Struct* 2003; 61: 265–270.
- [19]. Maimi P, Camanho PP, Mayugo JA. A continuum damage model for composite laminates: Part II–Computational implementation and validation. *Mech Mater* 2007; 39: 909–919.
- [20]. Bai Y, Keller T, Vallee T. Modeling of thermo-physical properties and thermal responses for FRP composites in fire. Asia-Pacific Conference on FRP in Structures. APFIS; 2007.
- [21]. Jae Hun Lee, Kwang Seok Kim, Hyo Kim. Determination of kinetic parameters during the thermal decomposition of epoxy/carbon fiber composite material. *Korean J Chem Eng* 2013; 30: 955–962.